

# SRM Design For Starter-alternator System

M. Besbes, M. Gabsi,  
E. Hoang, M. Lecrivain,  
B. Griani

Laboratoire d'Electricité  
Signaux et Robotique  
(LESiR CNRS UPRESA 8029)  
ENS Cachan,  
61, av. du Président Wilson,  
94325 Cachan Cedex, France.  
Tel. +33 (0)1 47 40 21 09  
Fax +33 (0)1 47 40 21 99  
E-mail:

C. Plasse

VALEO Systèmes Electriques,  
2, rue André Boulle - BP 150 –  
94004 Créteil

## ABSTRACT

This paper deals with the design of starter-alternator system integrated to a car flywheel based upon SRM technology. We discuss the feasibility of this application by comparing four different structures of SRM. We particularly underscore the effect of the pole number in electromagnetic performances and vibrational characteristics. In addition, a parametric analysis will be exposed to optimise the choice of the machine geometry and the choice of the turn number. Finally, we present a comparison between experimental results and simulations.

**Keywords:** SRM, starter-alternator system, parametric analysis, pole number.

## 1 INTRODUCTION

The power demand in cars is continuously increased. This requirement, associated to the anti-pollution norms, necessitates an optimised exploitation of energy. The starter alternator system integrated to flywheel can represent an attractive solution. It will have the following functions:

- + starting the thermal engine,
- + charging the car battery,
- + assisting the engine in accelerating,
- + stop-and-go function for urban traffic.

In this paper, we present a study about the feasibility of a integrated starter-alternator flywheel with a doubly salient switched reluctance machine rated. This machine is directly mounted on the crankshaft between the clutch and the thermal engine (Figure1). It is supplied by a battery of 36 Volts at starting mode and operates for alternator mode at 42 Volts network. We establish a comparison between different structures where we discuss the influence of the tooth number. A parametric study is performed to determine the optimal geometry able to produce the recommended performances, for both starter and alternator functions. We also study the hole

system (machine associated to its inverter) where the turn number and the control angles are optimised

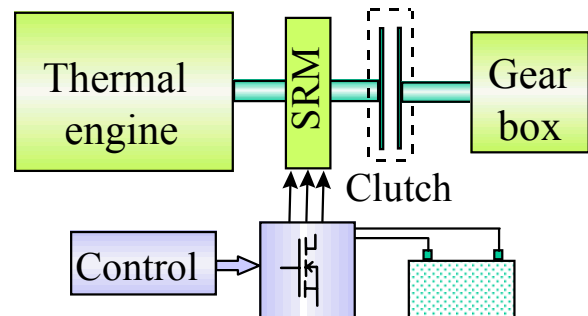


Fig. 1. System overview.

The SRM was chosen for its simplicity, robustness, high speed capability. It is successfully used in many applications such as: electric traction, starter-generator for aircraft engine [1,2], high speed application ...

## 2 ELECTROMAGNETIC CHARACTERISTICS

The requirements of the machine, which should replace the starter and the alternator into one unit, are particularly characterised by a high torque (quite 150 Nm) for starting and a constant power generation from 1,000 rpm up 6,000 rpm. The volume of this machine is very limited specially the frame length. The starting torque can be obtained only with high m.m.f. where the saturation is important and the limit of energy conversion can be reached. For SRM with high tooth number, the saturation influence will be limited due to the reduction of the flux path [3] and the converted energy will increase. In addition, the winding overhang becomes smaller and a longer stack will be possible.

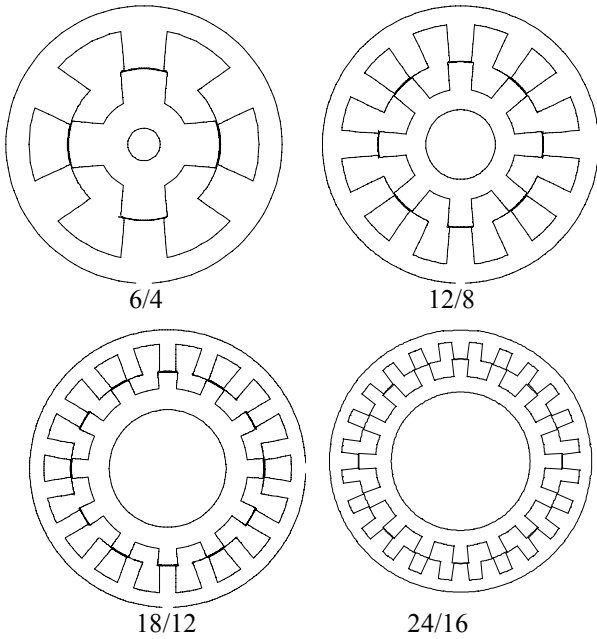


Fig. 2. Cross section of the studied machines.

Figure 3 presents magnetic flux per pole versus m.m.f. from aligned position to unaligned position. It shows the capability of the energy conversion of each structure.

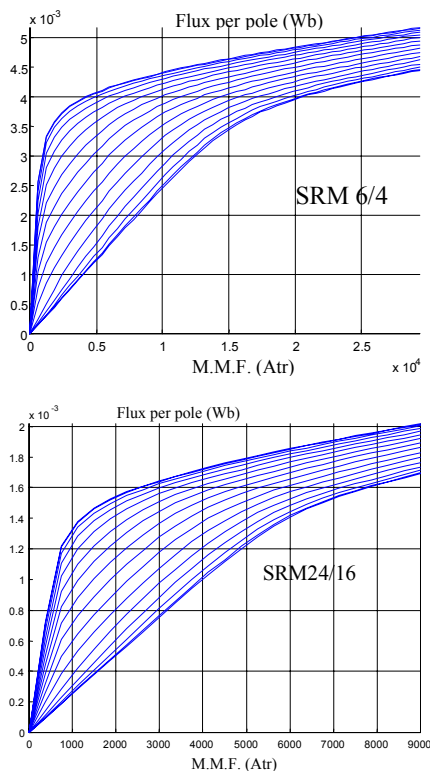


Fig. 3. Magnetic characteristics.

For the same stack length and the same air-gap, the torque produced by a machine of high pole number per phase is more important at the same copper losses.

### 3 OPTIMISATION OF GEOMETRIC PARAMETERS

We define two non-dimensional parameters:  $k_c$  as the ratio between the yoke thickness and the half of a stator pole width, and  $k_r$  as the ratio between the air-gap diameter and the external diameter. In order to increase the production of the starting torque, we perform a calculation of the maximum torque as function of  $k_c$  and  $k_r$  with the same current density (figure 4 for 18/12 SRM).

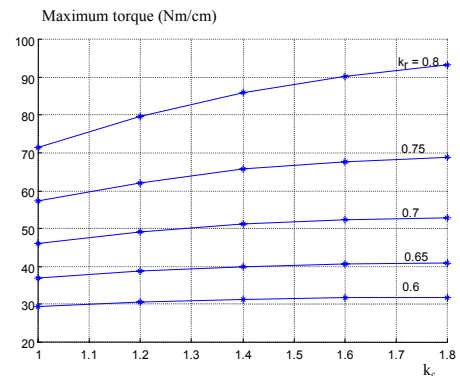


Fig. 4. Maximum torque of a 18/12 SRM as a function of  $k_c$  for different value of  $k_r$ .

The final choice of a geometry must take into account the different kinds of losses. The increase of the yoke thickness is favourable for: the decrease of iron losses as well as vibrations and acoustic noise of magnetic origin, the improvement of the starting torque ...

We can also note that increasing the 'pitch angle'  $\alpha$  can improve the torque production. We choose this angle for the tested machine in such way that the winding area will not be reduced for a coil rectangular shape [4].

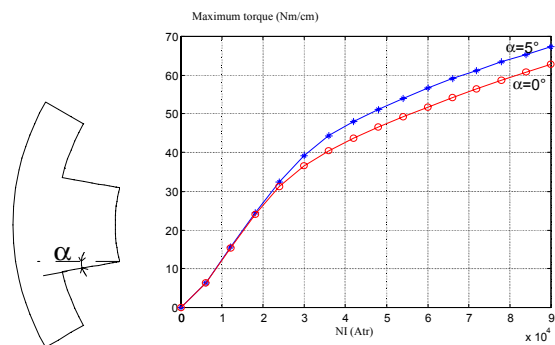


Fig. 5. Maximum torque as function of m.m.f. for different values of  $\alpha$ .

### 4 CHOICE OF TURN NUMBER

In general, the turn number is chosen at the rated speed. For this choice, the machine produces the needed torque at low speed and the specified power at maximum speed. At 100 rpm, we compute the electromagnetic torque as function of turns for different values of firing angle  $\psi$  and magnetisation angle  $\theta_p$ .

Figures 6 and 7 clearly show that the produced torque is maximum with a turn number equals to 10 in the case of a 18/12 SRM.

Torque ripple will be minimised with a adequate choice of angle control and a current reference. However, in order to improve the performances at high speed for alternator function, we should reduce the turn number. This implies an increase of current to produce the starter torque. In consequence, the battery will be hardly solicited and the currents constraints will be more important.

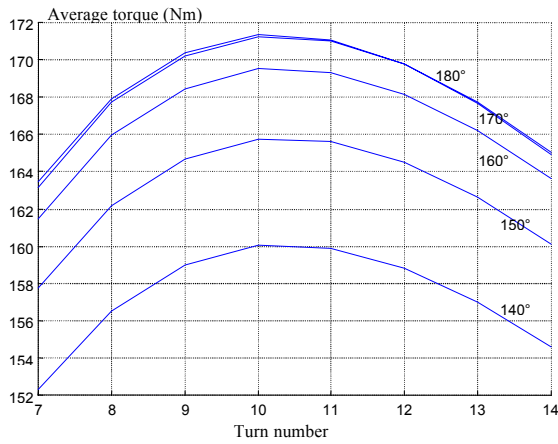


Fig. 6. Average torque as function of turn number for different value of magnetisation angle (firing angle = 0°).

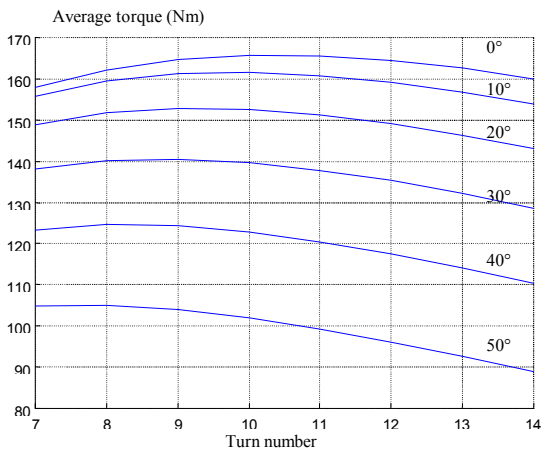


Fig. 7. Average torque as function of turn number for different value of firing angle (conduction angle = 180°).

## 5 STARTER AND GENERATOR FUNCTIONS

The studied machines have three phases and supplied with an inverter as presented in figure 8. We consider that the phases are de-coupled and the simulation is done with a single phase.

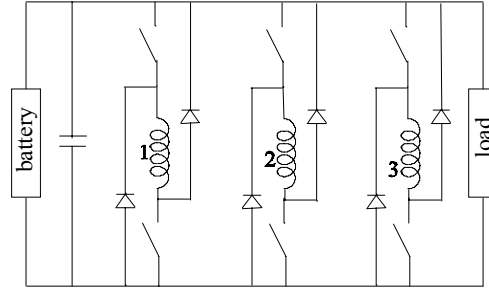


Fig. 8. Converter topology.

We compute the magnetic flux and the static torque for different current values and rotor positions by using a finite element analysis. These computations take into account the saturation phenomena and the rotor movement. The different steps of computations are described in figure 9:

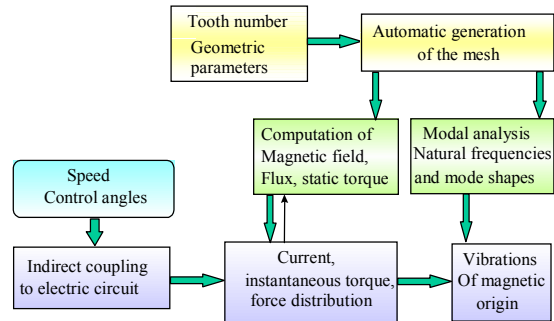


Fig. 9. Different steps of computation.

The SRM is directly mounted to the crankshaft without velocity gear ratio. The SRM must produce the starting torque in each rotor position. Figure 10 presents the maximum torque (for a locked rotor test) that the machine can produce for different rotor positions. This figure shows for each position which phases should be supplied (with one phase or two phases) in order to obtain a torque greater than 140 Nm.

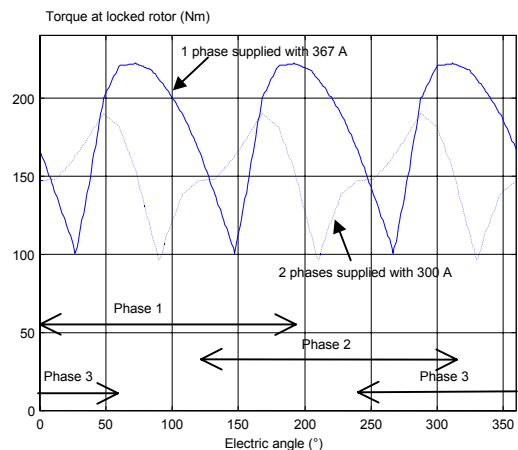


Fig. 10. Maximum static torque as a function of rotor position at constant current.

The SRM generator function is mainly tied to the firing angle. The machine operates with two steps: the first corresponds to a phase magnetisation where the current flows from the battery to the coils and the second corresponds to a phase demagnetisation where the machine delivers energy to charge the battery. At 2,000 rpm, the average value of the DC bus current as a function of  $\psi$  and  $\theta_p$ , always presents a extreme value (fig. 10) for both motor operating and alternator operating. For  $\theta_p = 180^\circ$ , the delivered current as well as its ripples are the most important.

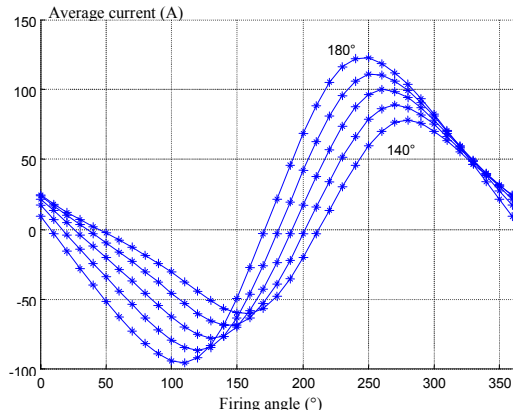


Fig. 11. Average values of generator current as function of firing angle for different values of magnetisation angle.

The wave form of the average current versus the firing angle is not symmetric because of the non-symmetry of the rectifier. For starting, the control angles, associated to the current reference, are chosen such as the torque ripples are minimised. However, for generator operating, the control is optimised to deliver the needed power with respect to a high efficiency and a minimum ratio between excitation energy and generated energy [5].

## 6 VIBRATIONAL CHARACTERISTICS

The study of vibrational behaviour of SRM is especially based on the determination of modal characteristics (natural frequencies and mode shapes) of the stator. Only first modes are the main sources of nuisance and particularly when harmonic frequencies of magnetic forces coincide with natural frequency of the structure [6]. For three-phased machines, mode shapes of rank  $N_s/3$  ( $N_s$ : stator tooth number) will be excited with harmonic forces of rank  $3k \pm 1$ ; and mode shapes of rank  $N_s$  as well as the aspiration mode (or mode zero) will be excited by harmonic forces of rank  $3k$  [7,8].

The calculation of natural frequencies of these different structures of SRM shows that increasing the pole number is accompanied by a decrease of natural frequencies. However, the number of resonance frequencies in the audible spectrum is consequently increased. On the other hand, the first modes, which are susceptible to be excited by harmonic forces of rank  $3k \pm 1$ , will have higher natural frequencies.

Table 1. Natural frequencies (Hz) of the stator.

Mode order	SRM 6/4	SRM 12/8	SRM 18/12	SRM 24/16
2	900	678	509	327
3	2087	1792	1381	895
4	4263	3145	2518	1654
5	5806	4463	3823	2559
6	7201	5339	5176	3559
7	9020	7782	6415	4594
8	13872	8903	7326	5592
0	5476	5124	5328	4903

In addition, this computation proves that aspiration modes associated to these different machines have almost the same frequency. In fact, this mode mainly depends on the external diameter which is held constant.

## 7 EXPERIMENTS AND COMPARAISON

According to geometric constraints (in particular the shaft diameter) and electromagnetic specifications, a 24/16 SRM is chosen as a tested machine (fig. 12). We present in this paper only the starting mode performances.



Fig. 12. the tested machine.

At a given rotor position, we measure the phase current and the produced torque. The phase is supplied by a regulated voltage generator. The measure duration don't exceed 5 s in order to limit the increasing of the temperature. In this case, the phase resistance increases with the temperature and the current decreases from 300 A to 270 A. Table 2 shows a good concordance between measurements and finite element computation.

Table 2. Comparison of measurement and simulation of the static torque at a given position of the rotor.

Current (A)	270	280	290	300
Measured Torque (Nm)	158	164	168	172.5
Computed Torque (Nm)	158.2	163	169	175.2

For different speeds (from 100 rpm to 1,000 rpm), we measure the maximum average torque produced by the tested machine. These measurements show the ability of this structure to start the thermal engine and to accelerate it to idle speed (boost function).

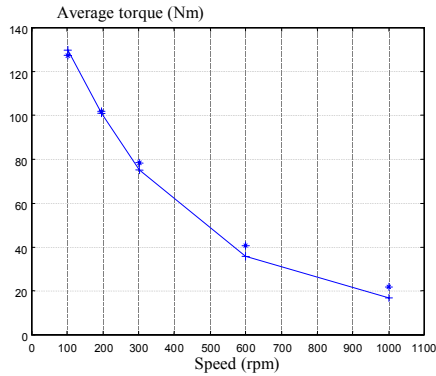


Fig. 13. Maximum average torque as a function of velocity (\* : simulations, + : measurements).

Compared to simulations, we observe a slightly difference at high speed. This is mainly due to iron losses, which are neglected in simulations, and also to the errors in computing unaligned inductance. In fact, the height of the studied machine is not important compared to its external diameter. So, a 2D computation can induce some errors neighbour unaligned position.

At 100 rpm, the machine can develop a torque equal to 130 Nm with a firing angle equal to  $-23^\circ$ , a magnetisation angle equal to  $160^\circ$  and a maximum value of the phase current which is quite equal to 250 A. Figures 14 and 15 show a good concordance between measurements and simulations of currents.

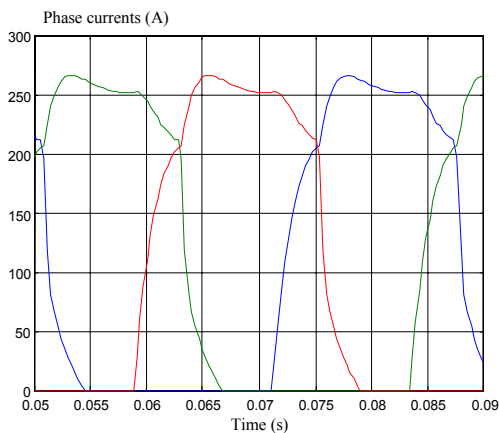


Fig. 14. Simulated wave-form of phase currents.

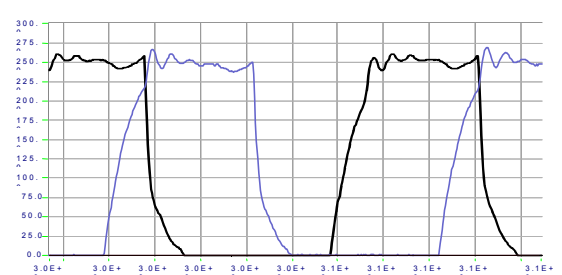


Fig. 15 Measurement current of phases 1 and 2.

## 8 CONCLUSION

This study presents a detailed analysis of the design of SRM for a car starter-alternator system integrated to the flywheel. This analysis is based upon a comparison of four structures of machines and proves that a 24/16 SRM is the most interesting. In this case, the saturation level is less important and the energy conversion is improved. In addition, the current constraints in the DC bus (battery) will be limited. This choice implies a high electric frequency and thus leads to produce high iron losses. However, from 1,000 rpm, the machine is used as alternator, and it is supplied with a voltage control. So the iron losses can decrease when the speed increases.

A model analysis of stator with different pole number proves that the fundamental mode (of rank  $N_s/3$ ) has a high natural frequency on one hand, and on another hand will be excited with harmonic magnetic forces of high order. In consequence, vibrations of magnetic origin can be reduced.

An investigation of the alternator operating of the tested machine, rated at 5 kW, is working in progress. Experimental results and simulations will be presented in a future paper .

## REFERENCES

- [1] Stephen R. MacMinn and William D. Jones, 'A very high speed switched-reluctance starter-generator for aircraft engine applications', IEEE IAS 1989, pp 1758-1764.
- [2] E. Richter, "Design and performances simulation for a gas turbine integrated starter/generator", Proceeding of ICEM'98, September 1998, pp. 2116-2121.
- [3] Lovatt H. C. and Stephenson J. M., 'Influence of number of poles per phase in switched reluctance motors', IEE proceedings-B, Vol. 139, N°4, July 1992.
- [4] E. Hoang, B. Multon, R. Vives Fos and M. Geoffroy, "Influence of stator yoke thickness and stator teeth shape upon ripple and average torque of switched reluctance motors", Proceeding of SPEEDAM, June 1994, pp. 145-149.
- [5] Kjaer P. C., Cossar C., Gribble J.J., Li Y. and Miller T.J.E. 'Switched reluctance generator control using an inverse machine model', Proceeding of ICEM, pp. 380-385, 1994.
- [6] Besbes M., Ren Z., Razeq A. and Allano S. , 'vibration diagnostic for doubly salient variable reluctance motor', International Conference on Electrical Machines (ICEM), 1994, 3, pp. 415-418.
- [7] Sadowski N., Lefèvre Y., Neves C.G.C. and Carlson R. : 'Finite elements coupled to electrical circuit equations in the simulation of switched reluctance drives: attention to mechanical behaviour,' IEEE Transaction on Magnetics, 1996, 32, (3), pp. 1086-1089.
- [8] M. Besbes, C. Picod, F. Camus and Gabsi M. : 'Influence of stator geometry upon vibratory and electromagnetic performances of SRM', IEE Proceeding Electric Power Application, Vol. 145, No. 5, septembre 1998, pp. 462-468